Signal subspace comparison between physical & synthesized array data in echo imaging

Jeong-Hee Choi, Ph. D.
School of Computer & Communication Engineering
Taegu University, Korea
Tel : 053-850-6632
Fax : 053-850-6619
E-mail : choijh@biho.taegu.ac.kr

In Synthetic Aperture Radar(SAR) imaging, the echoed data are collected by moving radar's position with respect to the target area, and this operation actually gives effect of synthesizing aperture size, which in turn gives better cross range resolution of reconstructed target scene. Among several inversion scheme for SAR imaging, we uses an inversion scheme which uses no approximation in wave propagation analysis, and try to verify whether the collected data with synthesized aperture actually gives the same support as that with physical aperture in the same size. To do this, we make a signal subspace comparison of two imaging models with physical and synthesized arrays, respectively. Theoretical comparison and numerical analysis using Gram-Schmidt procedures had been performed. The results showed that the synthesized array data fully span the physical array data with the same system geometry and strongly support the proposed inversion scheme valuable in high resolution radar imaging.

I Introduction

Unlike a traditional radar system, the new technology using Synthetic Aperture Radar(SAR) imaging system is capable of imaging a target as well as ranging and detection of the target. This imaging radar system employs synthesizing aperture techniques instead of using huge size physical antennas by moving radar(SAR) or target(Inverse SAR) in echo data collection. Such echo imaging techniques applies to raw data processing of various remote sensing problems such as geophysical exploration, environmental monitoring, and reconnaissance of military purpose[1][2][3].

In this paper, we make a comparison of two imaging models which are called physical and synthesized arrays in echo imaging. Both of them have the same system geometry except that one uses physical fixed array as an aperture while the other synthesizes the same size of aperture through the Doppler processing. The inversion based on each model is a computationally manageable method that incorporates the radiation pattern of each element on the array at the transmit and receive modes. For this comparison, we use the inversion equation of synthetic aperture radar imaging[4] and that of physical aperture discussed detail in this paper.

This study indicates that a physical array and its synthesized counterpart possess the same *resolution* despite of the fact that the synthesized array's signal subspace is a subset of much larger signal subspace for the physical array. This study also shows that the data from physical array contains redundant information as compared with the synthesized counterpart.

II. System model and inversion with physical and synthesized array data

We consider the system model and the inversion for a monostatic and ground-plane physical array with a source of spherical radiation pattern(See Fig. 1). For

SAR, a monostatic radar is mounted on a vehicle such as an aircraft or satellite moving along certain prescribed pat, and transmit source and receive echo signal while it is moving[4]. Unlike the synthesized array, a physical array is a group of Single Element Transducers (SETs) fixed on the line and all SETs record returning signal from the object area at the same time for the one source of SETs. The system geometry is the same as that of the SAR system except that a group of SETs are fixed along the line $x=X_1$ in the (x, y) plane instead of moving a SET along the line. This physical array makes a transmission at (X_1, Y_1+u) and its corresponding reception at all SETs (X_1, Y_1+v) for $u \in [-L, +L]$, $v \in [-L, +L]$ on the (x, y) plane. The (x, y) coordinate represent range and cross range, respectively. The wave traveling in the medium surrounding the target has temporal frequency of ω and the source signal has certain bandwidth centered at carrier frequency.

Since the radar's radiation pattern at far field is spherical, the phase delays by a point scatterer at (x, y) for the transmit-mode and receive-mode are $k\sqrt{(X_1-x)^2+(Y_1+u-y)^2}$ and $k\sqrt{(X_1-x)^2+(Y_1+v-y)^2}$, respectively, when we assume we have physical array antenna.

Thus, the total recorded echoed signal from the target area at physical array is

$$p(u, v, \omega) = \int\int f(x, y) \cdot \exp[jk\sqrt{(X_1-x)^2+(Y_1+u-y)^2}] \exp[jk\sqrt{(X_1-x)^2+(Y_1+v-y)^2}]dx\ dy \quad (1)$$

where $f(x, y)$ is the object's reflectivity function. For notational simplicity, we consider the case of $Y_1=0$, i.e., broad side case.

The spherical wave with wavenumber k, i.e., $\exp[jk\sqrt{(X_1-x)^2+(u-y)^2}]$, has spectral decomposition of the SET's radiation pattern as follows:

$$\int_{-\infty}^{\infty} \frac{\exp[j(\sqrt{k^2-k_u^2}(X_1-x)+k_u(u-y)]}{\sqrt{k^2-k_u^2}}\, dk_u, \quad (2)$$

where k_u represents the *Fourier* transform pair of u. Similarly for v, we have

$$\int_{-\infty}^{\infty} \frac{\exp[j(\sqrt{k^2-k_v^2}(X_1-x)+k_v(v-y)]}{\sqrt{k^2-k_v^2}}\, dk_v, \quad (3)$$

where k_v represents the *Fourier* transform pair of v.
By substituting eq. (2) and eq. (3) in eq. (1) and after some rearrangement (amplitude suppressed), one obtains

$$p(u, v, \omega) = \int_{-\infty}^{\infty} dk_u \int_{-\infty}^{\infty} dk_v\ F(\sqrt{k^2-k_u^2}+\sqrt{k^2-k_v^2},\ k_u+k_v) \cdot \exp[j(\sqrt{k^2-k_u^2}+\sqrt{k^2-k_v^2})X_1]\ \exp[j(k_u u+k_v v)]. \quad (4)$$

Note that $F(*, *)$ is *Fourier* counterpart of $f(x, y)$. Taking the spatial Fourier

transform of both sides of eq. (4) with respect to u and v yields,

$$P(k_u, k_v, \omega) = F(\sqrt{k^2 - k_u^2} + \sqrt{k^2 - k_v^2},\ k_u + k_v)\ \exp[j(\sqrt{k^2 - k_u^2} + \sqrt{k^2 - k_v^2})X_1]. \quad (5)$$

Finally, from eq. (5) we can write the following inversion equation:

$$F(k_x, k_y) = \exp[-jk_x X_1]\ P(k_u, k_v, \omega), \quad (6)$$
$$\text{where } k_x \equiv \sqrt{k^2 - k_u^2} + \sqrt{k^2 - k_v^2} \text{ and } k_y \equiv k_u + k_v.$$

In the same geometry, the phase delay for Synthetic Aperture Radar is $2k\sqrt{(X_1 - x)^2 + (Y_1 + u - y)^2}$ and total recorded data from the point target located at (x, y) is represented as

$$s(u, \omega) = \int\int f(x, y) \cdot \exp[j\, 2k\sqrt{(X_1 - x)^2 + (Y_1 + u - y)^2}]\, dx dy. \quad (7)$$

The inversion equation is

$$F(k_x, k_y) = \exp[-jk_x X_1]\ S(k_u, \omega), \quad (8)$$
$$\text{where } k_x \equiv \sqrt{4k^2 - k_u^2} \text{ and } k_y \equiv k_u.$$

From eq. (6) and (8), the coverage of the temporal and spatial frequency domain data in the spatial frequency domain of target, i.e., $F(k_x, k_y)$, is depicted as Fig. 2 and Fig. 3.

III. Signal subspace comparison

A. Theoretical Study

Recall that $s(u, \omega)$ is the recorded data at the synthesized aperture. If there are N unique measurements made for a synthesized array, the number of unique data for a physical array is $\frac{N(N+1)}{2}$. Moreover, the signal subspace of a synthesized array is a subset of the signal subspace for a physical array of the same size. Despite this fact, the following clues raise the question of whether a physical array data contain redundant information or not.

- *Fact 1* : Fig. (2) and Fig. (3) based on the facts in eq. (6) and eq. (8), indicate that the spatial frequency coverage obtained via a physical array and a synthesized array of the same size are approximately identical.
- *Fact 2* : From the results in Ref. [4], it can be shown that the cross-range resolution in the broadside case for both the physical and synthesized arrays is $\Delta y = \frac{X_1 \lambda}{4L}$, where $\lambda = \frac{2\pi}{k}$ is the wavelength of the impinging field and L is half of the aperture size.
- *Fact 3* : The empirical studies show that the physical arrays yield images with cross-range resolutions that are slightly inferior to those of synthesized arrays of the same size. This can be attributed to the fact that the two-dimensional discrete Fourier transforms performed in the (u, v) domain for a physical array produces more

numerical errors than the one-dimensional discrete *Fourier* transform in u domain for a synthesized array.

In addition to the above Fact 1, 2 and 3, we can prove that physical array data for a point scatterer can be represented via a linear combination of the synthetic aperture data for the point scatterer. If we consider only one point target in the object region, that is, $f(x,y)=\delta(x-x_0, y-y_0)$, then the recorded signals using physical and synthesized arrays are

$$p(u,v,\omega)=\exp[jk\sqrt{(X_1-x_0)^2+(u-y_0)^2}]\ \exp[jk\sqrt{(X_1-x_0)^2+(v-y_0)^2}] \tag{9}$$

$$s(u,\omega)=\exp[j2k\sqrt{(X_1-x_0)^2+(u-y_0)^2}]. \tag{10}$$

By taking the *Fourier* transform of eq. (9) and eq.(10) in both (u,v) domain and spatially shift this data into object region by multiplying $\exp[-jk_xX_1]$ with an approximation of $X_1 \gg x_0$, we then obtain

$$P(k_u,k_v,\omega) \simeq A(k_u,k_v)\ \exp[-j\ (k_u+k_v)\ y_0], \tag{11}$$

$$S(k_u,\omega) \simeq B(k_u)\ \exp[-j\ k_u\ y_0], \tag{12}$$

where $A(k_u,k_v)=\dfrac{1}{\sqrt{k^2-k_u^2}\sqrt{k^2-k_v^2}}$ and $B(k_u)=\dfrac{1}{\sqrt{4k^2-k_u^2}}$.

Note that either $A(k_u,k_v)$ or $B(k_u)$ is an amplitude function.

From eq. (11) and eq. (12), we can represent $P(k_u,k_v,\omega)$ in terms of $S(k_u,\omega)$ for a fixed k_v. That is

$$P(k_u,k_v,\omega)\simeq C(k_u,k_v)S(k_u,\omega), \tag{13}$$

where $$C(k_u,k_v)=\frac{A(k_u,k_v)\exp(-jk_vy_0)}{B(k_u)}.$$

The total frequency coverage of the echoed data in (k_x,k_y) domain, consists of frequency coverage from each point target. In other words, the signal subspace of the Fourier domain data by one point target is a subset of the one by all point targets in the object region. Therefore, comparison of signal subspaces of physical and synthesized array data from one point target, gives the same conclusion in dealing with the total echoed signal subspace from the object area to be imaged. We also proved this relationship numerically next.

B. Numerical Study Using Gram-Schmidt Procedures

If an arbitrary vector $\bar{e}$ is in a signal subspace completely spanned by a set of orthonormal basis vectors, $\bar{\phi}_i$, where $i=1,..M$, then $\bar{e}$ can be completely represented by a linear combination of $\bar{\Phi}_i$'s. That is

$$\bar{e} = \sum_{i=1}^{M} \langle \bar{e}, \bar{\phi}_i \rangle \bar{\phi}_i,$$

where $\langle \cdot, \cdot \rangle$ represents the inner product of two vectors.

In the same manner, if each vector in the signal subspace of the physical array

data , i.e., $P(k_u, k_v, \omega)$, can be represented by a linear combination of orthonormal basis vectors, i.e, $\overline{\phi_i}$'s, induced from the synthesized array data, i.e., $S(k_u, \omega)$, then the size of the signal subspace from physical array data is the same as that from synthesized counterpart.

We use the Gram-Schmidt procedure to construct an orthonormal set of basis functions from the discrete two-dimensional synthetic aperture data, i.e., $S(k_u, \omega)$. We then project the discrete three-dimensional physical array data, i.e., $P(k_u, k_v, \omega)$ onto the signal subspace spanned by the orthonormal basis functions (or, equivalently, the synthetic aperture data). We then compare the obtained signal, i.e.,

$$\hat{P}(k_u, k_v, \omega) = \sum_{i=1}^{M} \langle P(k_u, k_v, \omega), \Phi_i \rangle \Phi_i$$

with the actual physical array data, i.e., $P(k_u, k_v, \omega)$. And the results showed that a linear combination of the orthonormal basis functions can produce a good estimate of the physical array data.

In our experiment, we used 64 samples in aperture $u \in [-256, 256]$ with sample spacing $\Delta_u = 8(meters)$ which satisfies the condition to avoid aliasing.[4] The object area which is centered at the origin is within the disk of radius $X_0 = 64$ $(meters)$ and the distance X_1 is $25600(meters)$. We used 64 temporal frequencies with $1/(4X_0)$ as a sample spacing of the wavenumber centered at 5π $(radians/m)$.

We estimate the physical array data from synthetic array basis functions for multi-target in the object area positioned at $(X_1, 0)$, $(X_1, 30)$, and $(X_1 + 30, -20)$. Fig. (4.a,b) shows actual and estimated physical array data in the k_u domain for a fixed k_v and temporal frequency. The SNR of the estimator is as good as 31.35 (db).

IV. Conclusion

We introduced an approximation free inversion scheme in SAR imaging and showed the synthesized aperture actually working as an physical antenna of the same size. This was proved by comparing signal subspace of physical and synthesized array data theoretically and numerically. The results showed that the synthesized array data fully span the physical array data with the same system geometry and strongly support the previously proposed inversion scheme valuable in high resolution radar imaging.

References

1) D. Ausherman, "Developments in radar imaging", *IEEE Trans. Aerospace and Electronic Systems*, 20:363, July 1984.
2) J. C. Curlander and R. N. McDonough, *Synthetic Aperture Radar*, New York: Wiley, 1991.
3) M. Soumekh, "Reconnaissance with ultra wideband UHF synthetic aperture radar," *IEEE Signal Processing Magazine*, vol. 12, no. 4, pp. 21-40, July 1995.
4) M. Soumekh, " Echo imaging using physical and synthesized arrays," *Optical Engineering*, vol. 29, no. 5, pp. 545-554, May 1990.
5) P. Morse and H. Feshbach, *Methods of Theoretical Physics*, New York: McGraw-Hill, 1968.
6) M. I Skolnik, *Introduction to Radar Systems*, New York: McGraw-Hill, 1980.

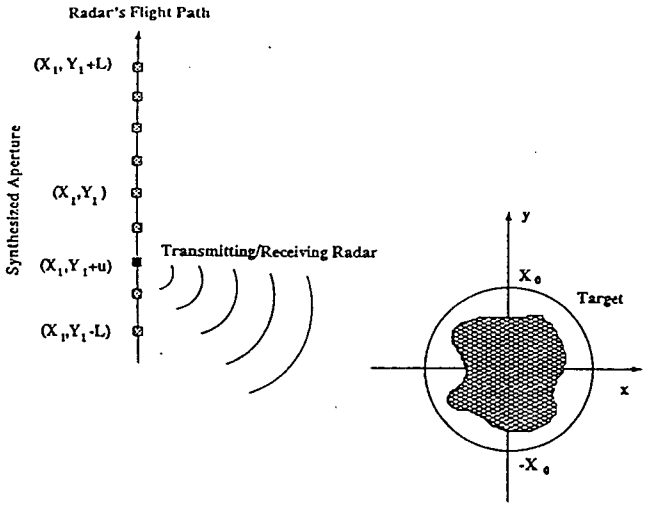

Fig. 1 Monostatic SAR Imaging system geometry

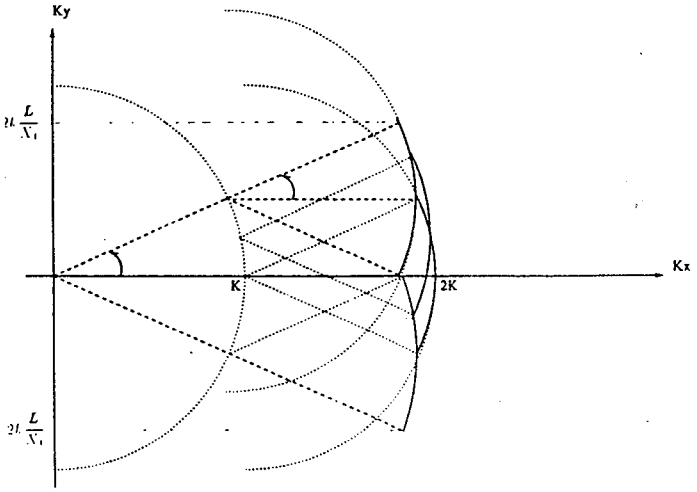

Fig. 2 Spatial frequency coverage of physical array data

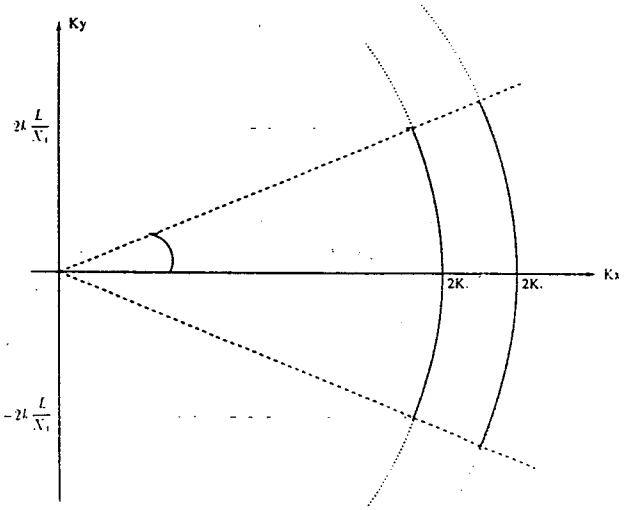

Fig. 3 Spatial frequency coverage of synthesized array data

Fig. (4.a)

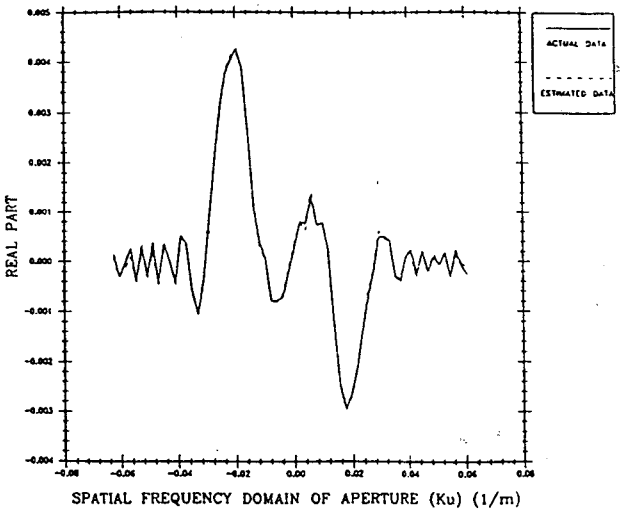

Fig. (4.b)

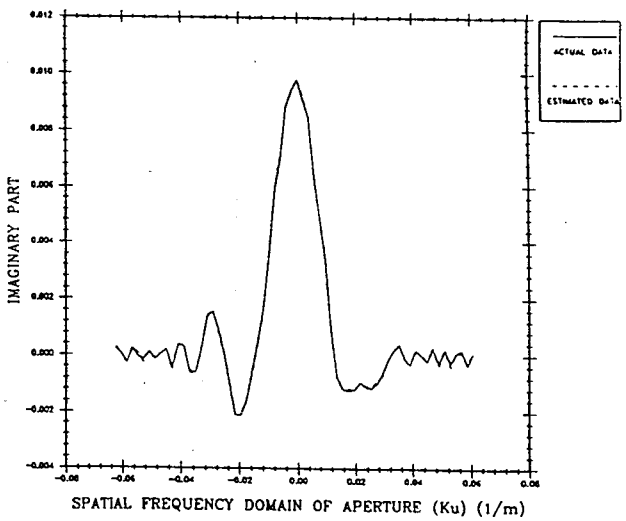

Fig. 4 a) Real part, b) Imaginary part, of estimated physical array data using SAR data basis for several random targets, SNR = 31.35 (db)